Geophysical Research Letters

RESEARCH LETTER
10.1029/2019GL084936

How Robust is the Atmospheric Response to Projected Arctic Sea Ice Loss Across Climate Models?

J. A. Screen[1,2] and R. Blackport[1]

[1]Department of Mathematics, University of Exeter, Exeter, Devon, UK, [2]Global Systems Institute, University of Exeter, Exeter, Devon, UK

Key Points:
- Wintertime atmospheric response to projected Arctic sea-ice loss can be well-estimated indirectly from CMIP5 simulations
- Robust changes across models including stronger Siberian High, weaker Icelandic Low, slower eddy-driven jet and faster subtropical jet
- Non-robust changes in surface air temperature over mid-latitude continents and sea level pressure over the North Pacific

Supporting Information:
- Supporting Information S1

Correspondence to:
J. A. Screen,
j.screen@exeter.ac.uk

Citation:
Screen, J. A., & Blackport, R. (2019). How robust is the atmospheric response to projected Arctic sea ice loss across climate models?. *Geophysical Research Letters*, *46*, 11,406–11,415. https://doi.org/10.1029/2019GL084936

Received 13 AUG 2019
Accepted 2 OCT 2019
Accepted article online 18 OCT 2019
Published online 28 OCT 2019

Abstract We assess the reliability of an indirect method of inferring the atmospheric response to projected Arctic sea ice loss from CMIP5 simulations, by comparing the response inferred from the indirect method to that explicitly simulated in sea ice perturbation experiments. We find that the indirect approach works well in winter, but has limited utility in the other seasons. We then apply a modified version of the indirect method to 11 CMIP5 models to reveal the robust and non-robust aspects of the wintertime atmospheric response to projected Arctic sea ice loss. Despite limitations of the indirect method, we identify a robust enhancement of the Siberian High, weakening of the Icelandic Low, weakening of the westerly wind on the poleward flank of the eddy-driven jet, strengthening of the subtropical jet, and weakening of the stratospheric polar vortex. The surface air temperature response to projected Arctic sea ice loss over mid-latitude continents is non-robust across the models.

Plain Language Summary The continued melt of Arctic sea ice will likely affect weather and climate in places far from the Arctic. To better understand the far-flung implications of sea ice loss, scientists can perform bespoke climate model experiments in which sea ice is reduced, but all other climate drivers are fixed. In our paper, we test the reliability of an indirect method to infer the atmospheric response to sea ice loss, which makes use of a large set of climate model experiments originally performed for other purposes. We find that the indirect approach works well in winter, but not so well in other seasons. We then apply the indirect method to 11 climate models to reveal the robust and non-robust aspects of the wintertime atmospheric response to projected Arctic sea ice loss—the largest such comparison to date. We found that the models agreed on quite a few aspects of the response, including warming over the Arctic, regional surface pressure changes over Siberia and Iceland, and a slowing of the mid-latitude jet stream. On the other hand, the models disagreed on whether surface air temperatures over Europe, North America, and East Asia will warm or cool in response to future Arctic sea ice loss.

1. Introduction

It is often said "what happens in the Arctic doesn't stay in the Arctic". The essence of this trope is that climate change in the Arctic, exemplified by the dramatic retreat of Arctic sea ice cover (Stroeve & Notz, 2018), affects weather and climate in places further south. That sea ice loss *can* affect weather and climate at lower latitudes is well established, but exactly *how* sea ice loss may impact the large-scale atmospheric circulation remains unclear (e.g., Barnes & Screen, 2015; Cohen et al., 2014; Vavrus, 2018). Many modelling studies have sought to address this question by performing sea ice perturbation experiments (e.g., Blackport & Kushner, 2016; Blackport & Screen, 2019; Deser et al., 2010; Deser et al., 2015; England et al., 2018; McCusker et al., 2017; Ogawa et al., 2018; Oudar et al., 2017; Peings & Magnusdottir, 2014; Smith et al., 2017; Screen et al., 2013; Sun et al., 2015; Sun et al., 2018), but most consider only a single model or the *average* of multiple models. The relatively few efforts to synthesize and compare results between climate models have revealed some common features of the atmospheric response to projected Arctic sea ice loss, but also substantial discrepancies across models (e.g., Hay et al., 2018; Screen et al., 2018). The largest comparison of sea ice perturbation experiments to date was conducted by Screen et al. (2018), which collated simulations from five models.

The advantage of sea ice perturbation experiments is that, with sea ice loss as the only forcing, they can be used to cleanly isolate the response to sea ice loss from that of other climate drivers. Although many modelling groups have performed such experiments, few have made the output freely available, hindering comparisons between models. Zappa et al. (2018), referred to as Z18 hereafter, introduced an indirect approach to

infer the atmospheric response to sea ice loss, leveraging publicly available simulations conducted as part of the Coupled Model Intercomparison Project phase 5 (CMIP5). Although the CMIP5 simulations were not designed for this express purpose, Z18 provide strong reasoning that their approach is able to disentangle the atmospheric response to sea ice loss from that to other climate drivers.

The purpose of this paper is twofold. First, we assess the suitability of the Z18 approach to estimating the response to sea ice loss, by comparing the response inferred from it to that explicitly simulated in sea ice perturbation experiments. Z18 did not formally test their method in this way. Second, we apply a modified version of the Z18 method to estimate the wintertime atmospheric response to projected Arctic sea ice loss from 11 CMIP5 models, the largest comparison of its kind to date, to reveal the robust and non-robust aspects of the response. Whilst Z18 focussed on the multimodel mean response and in particular, that of the North Atlantic jet, we delve deeper into the responses simulated by individual models and the similarities and differences in these model-specific responses.

2. Data and Methods

2.1. CMIP5 Simulations

We make use of five experiments from the CMIP5 (Taylor et al., 2012), named *historical*, *rcp85*, *amip*, *amipFuture,* and *amip4xCO2*. Eleven models in CMIP5 archive had data for all five required experiments (supporting information, Table S1). The *historical* experiment is run with external forcing (greenhouse gas concentrations, ozone, aerosols, solar forcing, land use change, and so on) following observed values from 1850 to 2005. The *rcp85* experiment is run with projected external forcing from 2006 to 2100, following a high-end emissions scenario. The *historical* and *rcp85* experiments were performed with fully coupled climate models, which simulate interactions between the atmosphere, land, ocean, and sea ice. The *amip*, *amipFuture*, and *amip4xCO2* experiments were performed with prescribed sea surface temperature (SST) and sea ice concentration (SIC) and therefore, lack coupling between the atmosphere, ocean, and sea ice. In the *amip* experiment, the external forcing was the same as in the *historical* experiment, but the SST and SIC were prescribed to follow observed values from 1979 to 2008. The *amip4xCO2* experiment was analogous to the *amip* experiment, except that the CO_2 concentration was quadrupled. In the *amipFuture* experiment, the external forcing was the same as in the *amip* and *historical* experiments, but the prescribed SST had an additional warming pattern added. This warming pattern was derived from the average of 13 CMIP3 models at the time of CO_2 quadrupling and was scaled to have a global mean SST increase of 4 K averaged over the ice-free oceans (Bony et al., 2011; Webb et al., 2017). In both the *amipFuture* and *amip4xCO2* experiments, SIC were the same as in the *amip* experiment.

2.2. Diagnosing the Response to Sea Ice Loss

The Z18 approach takes advantage of the fact the sea ice is the same in the *amip*, *amipFuture*, and *amip4xCO2* experiments. They estimated the response to quadrupled CO_2 concentrations (hereafter, R_{CO2}), in the absence of sea ice loss, by subtracting the time average (1979–2008) from *amip* simulations from that in the *amip4xCO2* simulations, and the response to warming SSTs (R_{SST}) by subtracting the time average *amip* simulations from that in the *amipFuture* simulations. The total climate change response (R_{ALL}), including the direct radiative effects of increased CO_2, the effects of warming SST and of sea ice change, was estimated by subtracting the time average over the period 1975–2005 from the *historical* experiment from that over the period 2069–2099 in the *rcp85* experiment. Lastly, the response to sea ice loss (R_{ICE}) was inferred as the residual term after subtracting the sum of R_{SST} and R_{CO2} from R_{ALL}:

$$\mathrm{R_{ICE}} = \mathrm{R_{ALL}} - (\propto_{\mathrm{CO2}} \mathrm{R_{CO2}} + \propto_{\mathrm{SST}} \mathrm{R_{SST}}),$$

where $\propto_{CO2}$ and $\propto_{SST}$ are scaling factors, which account for the SST increase in *amipFuture* (relative to *amip*) and the CO_2 increase in *amip4xCO2* (relative to *amip*) being larger that in *rcp85* (relative to *historical*). Z18 computed $\propto_{SST}$ from the multi-model mean difference in tropical (30 °S–30 °N) SST between R_{ALL} and R_{SST}, which was 0.594. $\propto_{CO2}$, was set to 0.587, derived from difference in CO_2 radiative forcing between R_{ALL} and R_{CO2}.

The Z18 approach makes a number of assumptions. Foremost of these are that R_{SST}, $R_{CO2,}$ and R_{ICE} are separable and linearly additive; that R_{SST} scales linearly with the magnitude of tropical SST warming; that

R_{CO2} scales linearly with radiative forcing; and that R_{SST} and R_{CO2} are independent of the mean background state, which may differ between coupled and uncoupled versions of the same model (Smith et al., 2017), or the absence of atmosphere-ocean-ice coupling in the *amip*-type experiments. Z18 argued that these assumptions are approximately satisfied, but did not explicitly test them. Here, we compare the response to sea ice loss inferred from the Z18 approach to that simulated in sea ice perturbation experiments, which enables us to test the validity of these assumptions.

We made a few minor modifications to the Z18 approach. First, whereas Z18 used only one realization per model, we used ensemble means from all available realizations (Table S1). This modification led to a better estimate of the circulation response to sea ice loss, presumably due to improved separation of forced response from internal variability. For example, the pattern correlation between the inferred and simulated winter mean sea level pressure (MSLP) responses increased from 0.56 to 0.69 and 0.28 to 0.66 for HadGEM2-ES and CCSM4, respectively. Second, whereas Z18 calculated $\propto_{SST}$ based on the multi-model mean (i.e., it had a single value), we calculated $\propto_{SST}$ separately for each model. This allows us to diagnose R_{ICE} for each individual model and to assess its robustness across the 11 models. We note that $\propto_{SST}$ varied from 0.54 to 0.87 across the models. Third, we computed R_{ALL} using slightly different time periods: 1980–1999 for *historical* and 2080–2099 for *rcp85*. This required a slightly higher value of $\propto_{CO2}$ (0.628).

Our estimate of the inferred response to sea ice loss is derived as a residual from coupled model experiments and so, it includes effects of ocean coupling on the response to sea ice loss (see, e.g., Deser et al., 2015, 2016; Blackport & Kushner, 2018). However due to the pattern scaling ($\propto_{SST}$), we expect that any SST response to sea ice loss (e.g., Tomas et al., 2016; Wang et al., 2018) that projects onto the CMIP3-mean warming pattern and scales with tropical SST would be missed by our method and instead apportioned to SST change; as would any feedback of such sea ice-induced SST changes on the atmosphere (e.g., Blackport & Kushner, 2018; Cvijanovic et al., 2017). For this reason, we assume the inferred response will only be weakly influenced by ocean coupling and therefore, that it is reasonable to compare the inferred response to that simulated in atmospheric model simulations. In other words, just like atmospheric model simulations, we expect the Z18 method to only detect the direct atmospheric response to sea ice loss and not the response to sea ice-induced SST changes.

The *rcp85* experiment yields sea ice loss in both hemispheres. In this paper, we focus on the Northern Hemisphere and assume that the inferred response to sea ice loss is predominantly due to Arctic sea ice loss. To be clear, we do not rule out a Northern Hemisphere response to Antarctic sea ice loss in the coupled CMIP5 experiments, but we do not expect any such ocean-governed responses to be detected by the Z18 approach. Ayres and Screen (2019) performed an analogous analysis for the Southern Hemisphere response to Antarctic sea ice loss.

2.3. Sea ice Perturbation Experiments

To explicitly simulate the effects of sea ice loss, we performed atmospheric model simulations with prescribed SST and SIC. The use of atmosphere-only models enables us to prescribe exactly the same magnitudes and spatial patterns of sea ice loss as simulated in the CMIP5 experiments, ensuring a clean comparison. For this we used HadGEM2-A, which is the atmospheric component of the HadGEM2-ES model (Collins et al., 2011; Martin et al., 2011) and CAM4, which is the atmospheric component of the CCSM4 model (Gent et al., 2011). In the first experiment, we prescribed a repeating annual cycle of SST and SIC representative of the late 20th century (hereafter called the *amipSIChistorical*). These SST and SIC conditions were taken from the CMIP5 *historical* experiments of HadGEM2-ES (for the HadGEM2-A simulations) and CCSM4 (for the CAM4 simulations), averaged for the 1980–1999 period and across all available ensemble members. In the second experiment, we prescribed a repeating annual cycle of SIC representative of the late 21st century following the RCP8.5 scenario (hereafter called the *amipSICrcp85*). These SIC conditions were taken from the *rcp85* experiments, averaged over the 2080–2099 period and across all available ensemble members. The prescribed SST is the same in the *amipSICrcp85* and *amipSIChistorical* experiments, except for grid-boxes where the SIC differed between the two experiments. At these locations, the prescribed SST was taken from the *rcp85* experiments, averaged over the 2080–2099 period and across all available ensemble members. This procedure accounts for the local SST warming associated with reduced sea ice cover, but it excludes remote SST changes that are not directly tied to the ice loss (Screen et al., 2013). It also excludes remote SST changes driven by sea ice loss (e.g., Blackport & Kushner, 2018) to be

consistent with expectations that the Z18 approach will account for these in R_{SST} and not R_{ICE}. Both experiments were run for 260 years in each model. The response to sea ice loss was calculated by subtracting the time average of the *amipSIChistorical* experiment from that in the *amipSICrcp85* experiment. These simulations are the same as analyzed in Screen et al. (2015a, 2015b) and Ayarzagüena and Screen (2016), where further details on the models and experimental setup can be found.

3. Results

We begin by explicitly testing the Z18 method through comparison with purpose-designed sea ice perturbation experiments. Figure 1a shows the winter (December–January–February; DJF) near-surface air temperature response to projected Arctic sea ice loss in HadGEM2-ES inferred from the modified Z18 (hereafter, Z18m) approach. This inferred response can be compared to the simulated response to sea ice loss in HadGEM2-A (Figure 1b). The inferred and simulated responses are very highly similar, in both their spatial character (pattern correlation of 0.99) and magnitude, with widespread warming of more than 20 °C over the Arctic Ocean. A high level of consistency is also found between the inferred near-surface air temperature response from CCSM4 and that simulated by CAM4 (Figures 1c and 1d, respectively). For this model, the Z18m approach well captures the spatial pattern of the simulated response (pattern correlation of 0.98), but gives an underestimation of its magnitude.

The inferred winter 500 hPa geopotential height (Z500) response in HadGEM2-ES (Figure 1e) features elevated Z500 over the Arctic and reduced Z500 over Europe and the North Atlantic. These features are also seen in the simulated Z500 response in HadGEM2-A (Figure 1f). The inferred Z500 response displays some additional features in the North Pacific that are not captured in the simulated response. However, the pattern correlation between the inferred and simulated Z500 responses is 0.89. A lower pattern correlation of 0.63 is found between the Z500 response inferred from CCSM4 and that simulated by CAM4, with both showing elevated Z500 over the Arctic, with the maximum response over the eastern side of the Arctic Ocean. The inferred and simulated Z500 responses differ in sign over the North Pacific.

The winter MSLP response to sea ice loss inferred from HadGEM2-ES (Figure 1i) displays increased MSLP over Scandinavia and northern Russia and decreased MSLP across the North Atlantic, in the North Pacific, and over the Arctic Ocean. This inferred response pattern bears close resemblance (pattern correlation of 0.69) to that simulated in HadGEM2-A (Figure 1j) in response to sea ice loss. Comparing the MSLP response inferred from CCSM4 to that simulated by CAM4 (Figures 1k and 1l, respectively) reveals a similar level of consistency (pattern correlation of 0.66), with the Z18m approach well capturing the MSLP decrease over North America and the Sea of Okhotsk and the MSLP increase over Scandinavia and northern Russia. The main difference between the inferred and simulated-MSLP responses is found in the eastern North Pacific, where the inferred response from CCSM4 displays raised MSLP in contrast to decreased MSLP in the simulated response in CAM4.

The inferred and simulated zonal-mean westerly wind responses (Figures 1m–p) are similar in the troposphere (pattern correlations of 0.78 and 0.60, for HadGEM2 and CCSM4, respectively), but dissimilar in the stratosphere (pattern correlations of 0.30 and 0.04, respectively). The Z18m approach performs better for HadGEM2-ES than for CCSM4, for reasons that are unclear. A possible explanation is that HadGEM2-ES simulates a larger decline in Arctic sea ice compared to CCSM4 (see, e.g., Figure 1 in Screen et al., 2015a) and therefore, the response to sea ice loss may be easier to detect.

We have only considered the winter response to sea ice loss so far. Table S2 summarizes the performance of the Z18m approach, as measured by the pattern correlation between the inferred and simulated responses, for each season. For near-surface air temperature, we find pattern correlations of 0.9 or greater for both models in all seasons except summer. For Z500 and MSLP, the pattern correlations are generally higher in winter than in the other seasons. We conclude that the Z18m approach works well in winter, but has limited utility in the other seasons. We speculate that this seasonality reflects that the response to projected Arctic sea ice loss is strongest in winter (Deser et al., 2010, 2015) and therefore, more easily separable from other aspects of climate change (Blackport & Kushner, 2017; Hay et al., 2018; McCusker et al., 2017). Given the shortcomings of the Z18m approach outside of winter, we focus solely on winter in the remainder of the paper.

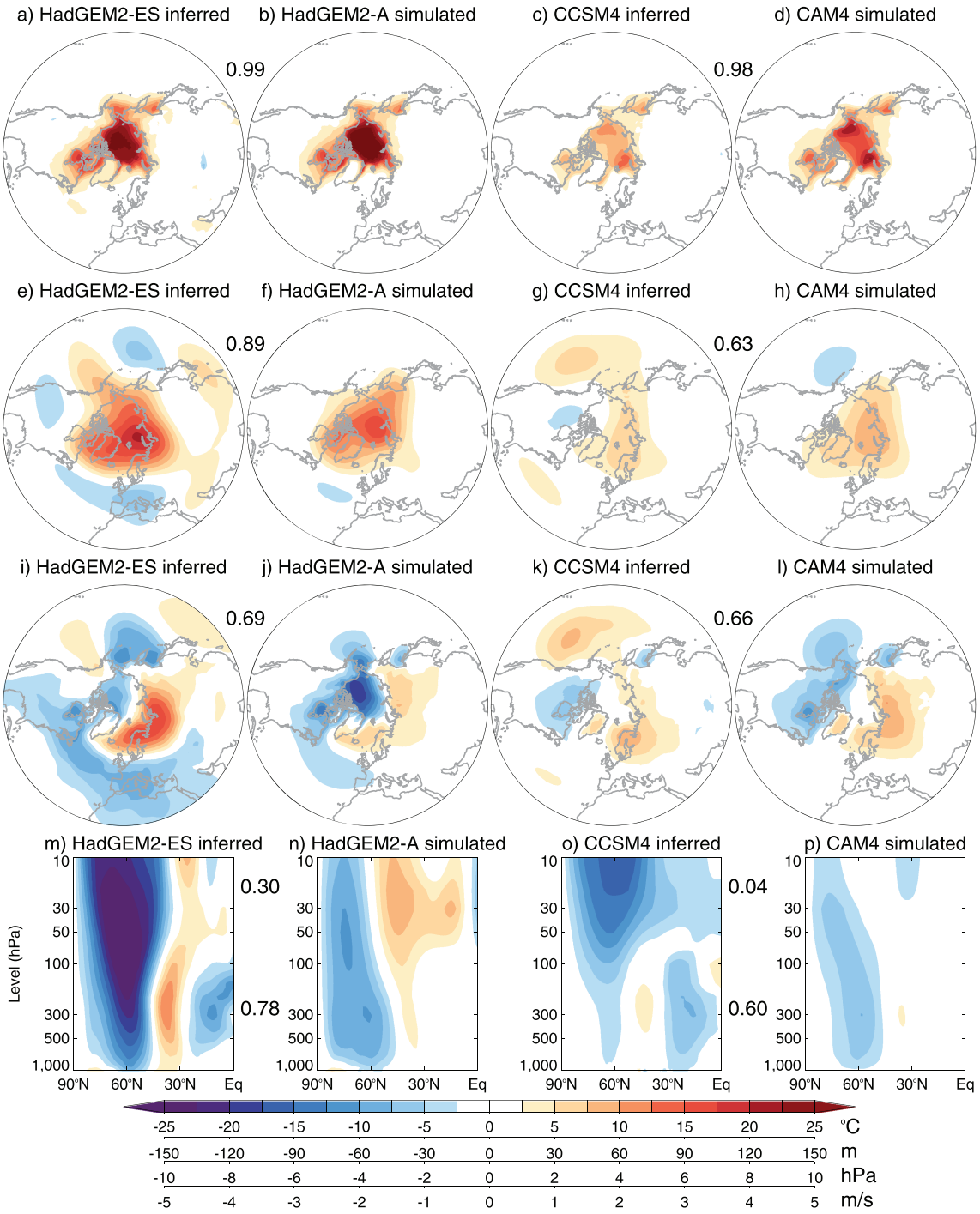

Figure 1. Winter (DJF) near-surface (1.5 m) air temperature response (a) as inferred from HadGEM2-ES and (b) as simulated by HadGEM2-A. (c) As a, but for CCSM4. (d) As b, but for CAM4. (e-h) As a–d, but for 500-hPa geopotential height. (i-l) As a–d, but for mean sea level pressure (hPa). (m-p) As a–d, but for zonal-mean westerly wind (m/s). The pattern correlation (calculated over latitudes 30–90 °N) is provided for each pair of inferred and simulated responses. In the bottom row, pattern correlations are shown separately for the troposphere (≥100 hPa) and stratosphere (<100 hPa).

Having demonstrated the ability of the Z18m approach to isolate the winter response to sea ice loss, we now apply the Z18m approach to output from 11 CMIP5 models in order to test the robustness of the response across models. Here, we define a robust response as being when 9 or greater of the 11 models depict individual responses of the same sign as the ensemble mean response. Figure 2 shows the winter near-surface air temperature response over land. All models simulate warming along the Arctic coast of Siberia and over

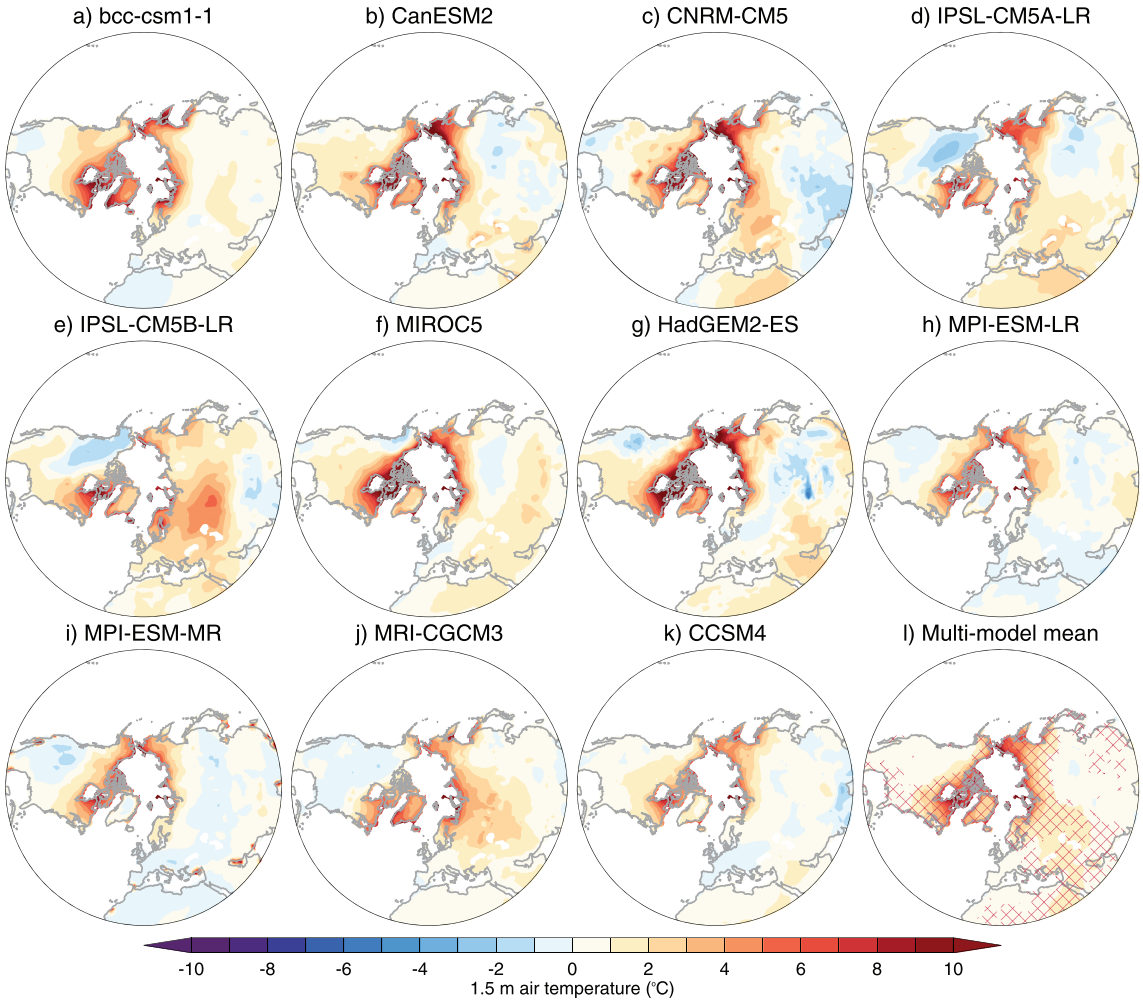

Figure 2. Winter (DJF) near-surface (1.5 m) terrestrial air temperature response to projected Arctic sea ice loss inferred from (a–k) eleven CMIP5 models and (l) the multi-model mean. Magenta hatching in (l) shows where nine or greater models agree on the sign of the response.

northeastern Canada, and most models show warming of Greenland, Scandinavia, and the eastern US. There is no consensus across the models on the sign of the temperature response over Europe, western North America, and East Asia. Several models display areas of cooling over central and/or east Asia, but of weak magnitude, supporting studies that suggest minimal influence of sea ice loss on wintertime Eurasian cooling (e.g., Blackport et al., 2019; McCusker et al., 2016; Sun et al., 2016) and the presence of and specific location of cooling is non-robust across the models.

The inferred winter MSLP response to sea ice loss is shown in Figure 3. The spatial pattern and magnitude of the MSLP response varies considerably across the models, although there are some common features. Most models display elevated MSLP over northern Siberia, reflecting an intensification of the Siberian High. However, this response is manifested more clearly and strongly in some models (e.g., HadGEM2-ES, CanESM2 and IPSL-CM5A-LR) and is absent in other models (e.g., bcc-csm1-1 and IPSL-CM5B-LR). In many models, the MSLP response projects onto the negative phase of the North Atlantic Oscillation (NAO), with elevated MSLP near Greenland and Iceland, and reduced MSLP over the mid-latitude Atlantic Ocean. The MSLP response most closely resembles the negative NAO in MIROC5 and HadGEM2-ES. None of the models analyzed here suggest a positive NAO response. The MSLP response over the North Pacific varies considerably between models and is non-robust. In this region, a full spectrum of responses is found from a strengthening of the Aleutian Low (e.g., HadGEM2-ES and MRI-CGCM3) to a weakening of the Aleutian Low (e.g., IPSL-CM5B-LR, MIROC5). Recall however, that the inferred and

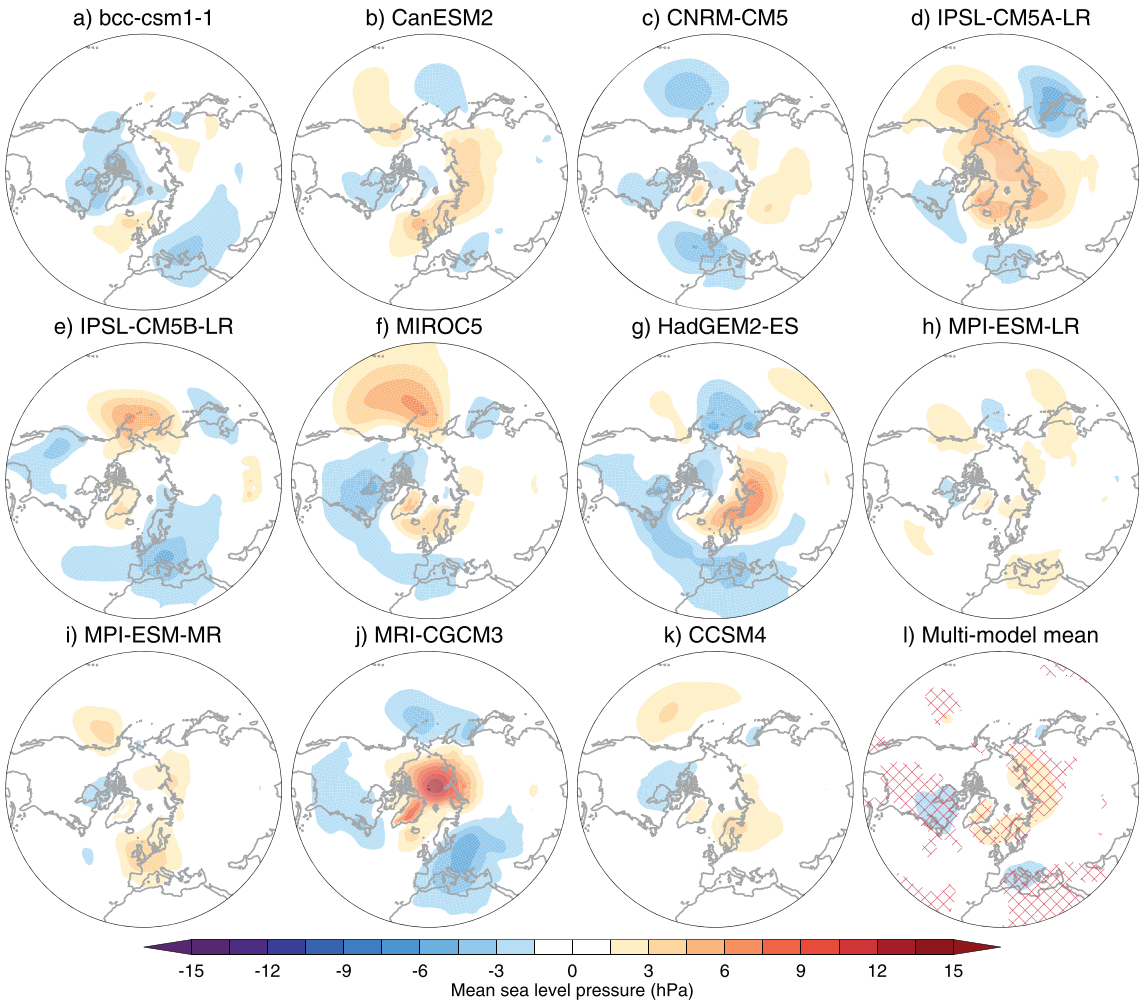

Figure 3. Winter (DJF) mean sea level pressure response to projected Arctic sea ice loss inferred from (a–k) eleven CMIP5 models and (l) the multi-model mean. Magenta hatching in (l) shows where nine or greater models agree on the sign of the response.

simulated MSLP responses in the North Pacific diverged in CCSM4 (Figures 1k and 1l), so the fidelity of the inferred MSLP responses in this region is questionable.

For Z500, there are robust increases in heights over high latitudes, but diverse responses in mid-latitudes (supporting information Figure S1). Lastly, Figure 4 shows the winter zonal-mean westerly wind response. There is general agreement across the models that the tropospheric westerly wind weakens at around 60 °N, on the poleward flank of the eddy-driven jet. The magnitude of this weakening varies considerably across the models. All bar one model (bcc-csm1-1) display weakened lower stratospheric westerly wind at 60 °N, and five models (CanESM2, IPSL-CM5A-LR, HadGEM2-ES, MPI-ESM-MR, MRI-CGCM3) show pronounced weakening of the westerly wind throughout the stratosphere, indicating a weakened polar stratospheric vortex. However, we again caution that the Z18m approach poorly captured the simulated stratospheric westerly wind response (Figures 1m–1p). The majority of models depict strengthened westerly wind in the upper troposphere at 30 °N, in the vicinity of the subtropical jet. The precise location and magnitude of this westerly wind increase varies, occurring in some models on the equatorward flank of the subtropical jet and in others, in the core or on the poleward flank of the subtropical jet. In summary, the inferred zonal-mean westerly wind responses suggest a robust weakening on the poleward flank of the eddy-driven jet, from the surface to the middle stratosphere and a robust strengthening in the vicinity of the subtropical jet (Figure 4l).

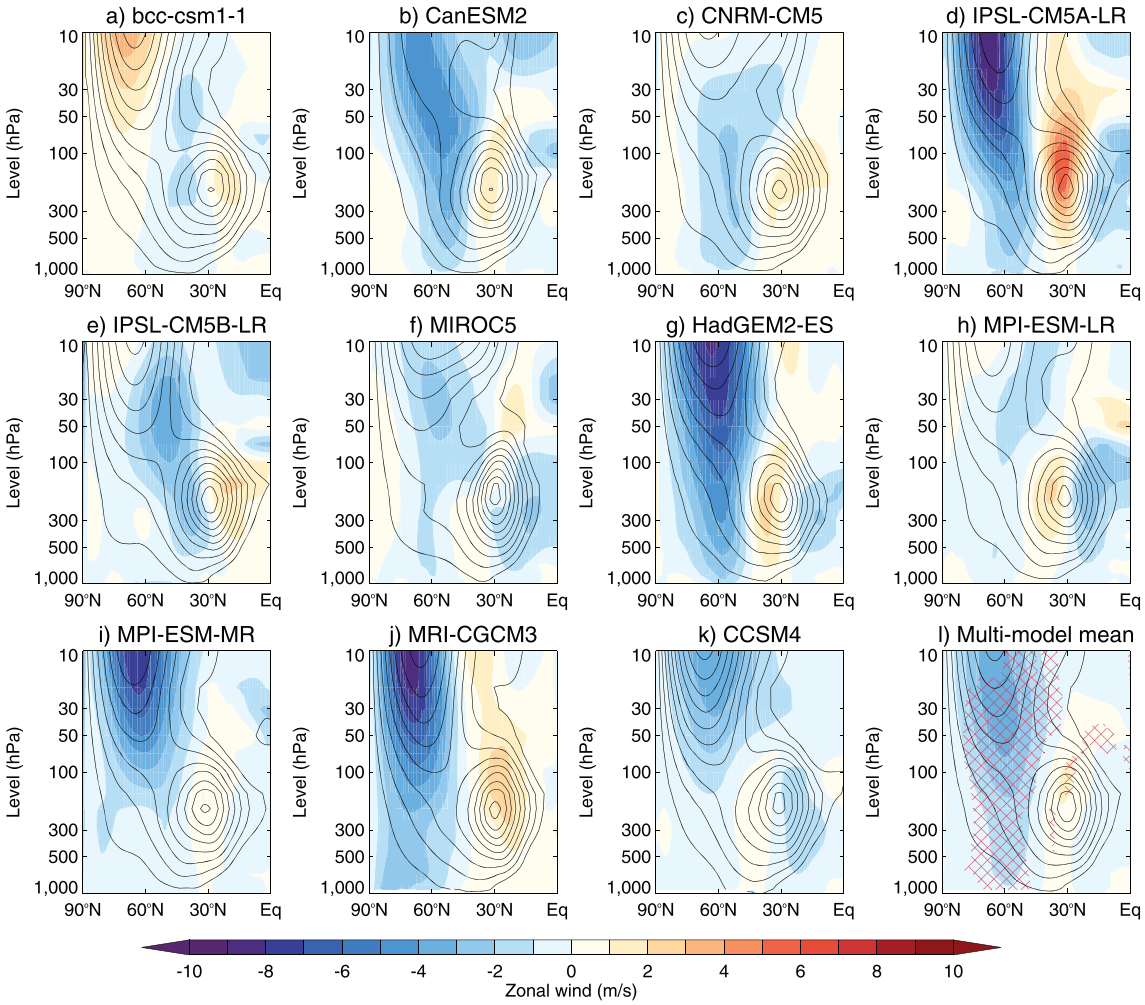

Figure 4. Winter (DJF) zonal-mean westerly wind response to projected Arctic sea ice loss inferred from (a–k) eleven CMIP5 models and (l) the multi-model mean. Black contours show the baseline climatology (contour interval of 10 m/s). Magenta hatching in (l) shows where nine or greater models agree on the sign of the response.

4. Discussion and Conclusions

We are mindful of several limitations of our indirect approach for inferring the response to sea ice loss, which need considering when interpreting the differences between models. Foremost of these is that the magnitudes and spatial patterns of projected Arctic sea ice loss differ between the models, and therefore, our results conflate uncertainty in the forcing (here, sea ice loss) and uncertainty in the forced response. Second, the pattern of SST change in each model is not identical to the CMIP3-mean pattern of SST change. This means that any atmospheric responses to SST changes that are spatially distinct from CMIP3-mean will be apportioned to sea ice loss (i.e., the residual term in our decomposition; see Methods) and not to SST change. Third, for some experiments, we have only a single ensemble member, which might not be a sufficiently large sample to fully separate the forced responses from internal variability; especially aspects of the response that have a low signal-to-noise ratio (Screen et al., 2014; e.g., in the polar stratosphere). Therefore, divergence between models arises partly due to the different magnitudes of spatial patterns of sea ice loss, varying spatial patterns of SST change, and internal variability. We suggest therefore, that our estimate of robustness of the response to sea ice loss is likely too low. Coordinated experiments with large ensembles and multiple models are underway to address these limitations, under the auspices of the Polar Amplification Model Intercomparison Project (Smith et al., 2019). The need for bespoke sea ice perturbation experiments is further underlined by the poor performance of the indirect method in seasons other than winter.

Despite these limitations, we have identified a number of features of the response that are qualitatively robust across the models. These are a surface warming at high latitudes (Figure 2l); enhancement of the Siberian High, particularly its northern edge (Figure 3l); weakening of the Icelandic Low, projecting onto the negative NAO (Figure 3l); weakening of the zonal wind on the poleward flank of the eddy-driven jet (Figure 4l); strengthening of the subtropical jet, albeit weaker in magnitude than the aforementioned change in the eddy-driven jet (Figure 4l); and weakening of the stratospheric polar vortex, at least in the lower stratosphere (Figure 4l). These features of the response are broadly consistent with past multi-model comparisons (e.g., Hay et al., 2018; Screen et al., 2018), but are corroborated here using a larger number of models. There is considerable model divergence of other aspects of the response. Most notably, there is lack of model agreement on the sign of the winter surface air temperature response over mid-latitude continents, including Europe, western U.S., and East Asia (Figure 2l) and of the MSLP response in the North Pacific (Figure 3l).

Acknowledgments
We thank the modelling groups that contributed to the CMIP5. The full CMIP5 data are freely available at the Climate Data Gateway https://www.earthsystemgrid.org. We thank Lantao Sun for providing the CAM4 simulations. The HadGEM2-A simulations were performed on the ARCHER UK National Supercomputing Service. This work was supported by grants from the Natural Environment Research Council (NE/R005125/1, NE/P006760/1) and the Leverhulme Trust (PLP-2015-215). A subset of post processed data, sufficient to replicate the published figures, is available at https://doi.org/10.24378/exe.1823 additional variables are available from the lead author upon reasonable request.

References

Ayarzagüena, B., & Screen, J. A. (2016). Future Arctic sea ice loss reduces severity of cold air outbreaks in midlatitudes. *Geophysical Research Letters*, *43*, 2801–2809. https://doi.org/10.1002/2016GL068092

Ayres, H., & Screen, J. A. (2019). Multimodel analysis of the atmospheric response to Antarctic sea ice loss at quadrupled CO_2. *Geophysical Research Letters*, *46*, 9861–9869. https://doi.org/10.1029/2019GL083653

Barnes, E. A., & Screen, J. A. (2015). The impact of Arctic warming on the midlatitude jetstream: Can it? Has it? Will it? *Wiley Interdisciplinary Reviews: Climate Change*, *6*, 277–286.

Blackport, R., & Kushner, P. J. (2016). The transient and equilibrium climate response to rapid summertime sea ice loss in CCSM4. *Journal of Climate*, *29*(2), 401–417.

Blackport, R., & Kushner, P. J. (2017). Isolating the atmospheric circulation response to Arctic sea ice loss in the coupled climate system. *Journal of Climate*, *30*(6), 2163–2185.

Blackport, R., & Kushner, P. J. (2018). The role of extratropical ocean warming in the coupled climate response to Arctic sea ice loss. *Journal of Climate*, *31*(22), 9193–9206.

Blackport, R., & Screen, J. A. (2019). Influence of Arctic sea ice loss in autumn compared to that in winter on the atmospheric circulation. *Geophysical Research Letters*, *46*, 2213–2221. https://doi.org/10.1029/2018GL081469

Blackport, R., Screen, J. A., van der Wiel, K., & Bintanja, R. (2019). Minimal influence of reduced Arctic sea ice on coincident cold winters in mid-latitudes. *Nature Climate Change*, *9*, 697–704.

Bony, S., Webb, M., Bretherton, C. S., Klein, S. A., Siebesma, P., Tselioudis, G., & Zhang, M. (2011). CFMIP: Towards a better evaluation and understanding of clouds and cloud feedbacks in CMIP5 models. *Clivar Exchanges*, *56*, 20–22.

Cohen, J., Screen, J. A., Furtado, J. C., Barlow, M., Whittleston, D., Coumou, D., et al. (2014). Recent Arctic amplification and extreme mid-latitude weather. *Nature Geoscience*, *7*(9), 627–637.

Collins, W. J., Bellouin, N., Doutriaux-Boucher, M., Gedney, N., Halloran, P., Hinton, T., et al. (2011). Development and evaluation of an Earth system model-HadGEM2. *Geoscientific Model Development*, *4*(4), 1051–1075. https://doi.org/10.5194/gmd-4-1051-2011

Cvijanovic, I., Santer, B. D., Bonfils, C., Lucas, D. D., Chiang, J. C., & Zimmerman, S. (2017). Future loss of Arctic sea-ice cover could drive a substantial decrease in California's rainfall. *Nature Communications*, *8*(1), 1947.

Deser, C., Sun, L., Tomas, R. A., & Screen, J. (2016). Does ocean coupling matter for the northern extratropical response to projected Arctic sea ice loss? *Geophysical Research Letters*, *43*, 2149–2157. https://doi.org/10.1002/2016GL067792

Deser, C., Tomas, R., Alexander, M., & Lawrence, D. (2010). The seasonal atmospheric response to projected Arctic sea ice loss in the late twenty-first century. *Journal of Climate*, *23*, 333–351.

Deser, C., Tomas, R. A., & Sun, L. (2015). The role of ocean-atmosphere coupling in the zonal-mean atmospheric response to Arctic sea ice loss. *Journal of Climate*, *28*(6), 2168–2186.

England, M., Polvani, L. M., & Sun, L. (2018). Contrasting the Antarctic and Arctic atmospheric responses to projected sea ice loss in the late twenty-first century. *Journal of Climate*, *31*(16), 6353–6370.

Gent, P. R., Danabasoglu, G., Donner, L. J., Holland, M. M., Hunke, E. C., Jayne, S. R., et al. (2011). The community climate system model version 4. *Journal of Climate*, *24*, 4973–4991.

Hay, S., Kushner, P. J., Blackport, R., & McCusker, K. E. (2018). On the relative robustness of the climate response to high-latitude and low-latitude warming. *Geophysical Research Letters*, *45*, 6232–6241. https://doi.org/10.1029/2018GL077294

Martin, G. M., Bellouin, N., Collins, W. J., Culverwell, I. D., Halloran, P. R., Hardiman, S. C., et al. (2011). The HadGEM2 family of Met Office Unified Model climate configurations. *Geoscientific Model Development*, *4*, 723–757.

McCusker, K. E., Fyfe, J. C., & Sigmond, M. (2016). Twenty-five winters of unexpected Eurasian cooling unlikely due to Arctic sea-ice loss. *Nature Geoscience*, *9*, 838–842.

McCusker, K. E., Kushner, P. J., Fyfe, J. C., Sigmond, M., Kharin, V. V., & Bitz, C. M. (2017). Remarkable separability of circulation response to Arctic sea ice loss and greenhouse gas forcing. *Geophysical Research Letters*, *44*, 7955–7964. https://doi.org/10.1002/2017GL074327

Ogawa, F., Keenlyside, N., Gao, Y., Koenigk, T., Yang, S., Suo, L., et al. (2018). Evaluating impacts of recent Arctic sea ice loss on the northern hemisphere winter climate change. *Geophysical Research Letters*, *45*, 3255–3263. https://doi.org/10.1002/2017GL076502

Oudar, T., Sanchez-Gomez, E., Chauvin, F., Cattiaux, J., Terray, L., & Cassou, C. (2017). Respective roles of direct GHG radiative forcing and induced Arctic sea ice loss on the Northern Hemisphere atmospheric circulation. *Climate Dynamics*, *49*, 3693–3713.

Peings, Y., & Magnusdottir, G. (2014). Response of the wintertime Northern Hemisphere atmospheric circulation to current and projected Arctic sea ice decline: A numerical study with CAM5. *Journal of Climate*, *27*(1), 244–264.

Screen, J. A., Deser, C., Smith, D. M., Zhang, X., Blackport, R., Kushner, P. J., et al. (2018). Consistency and discrepancy in the atmospheric response to Arctic sea-ice loss across climate models. *Nature Geoscience*, *11*(3), 155–163.

Screen, J. A., Deser, C., & Sun, L. (2015a). Projected changes in regional climate extremes arising from Arctic sea ice loss. *Environmental Research Letters*, *10*, 084006.

Screen, J. A., Deser, C., & Sun, L. (2015b). Reduced risk of North American cold extremes due to continued Arctic sea ice loss. *Bulletin of the American Meteorological Society*, *96*, 1489–1503.

Screen, J. A., Simmonds, I., Deser, C., & Tomas, R. (2013). The atmospheric response to three decades of observed Arctic sea ice loss. *Journal of Climate*, *26*(4), 1230–1248.

Screen, J. A., Simmonds, I., Deser, C., & Tomas, R. (2014). Atmospheric impacts of Arctic sea-ice loss, 1979-2009: Separating forced change from atmospheric internal variability. *Climate Dynamics*, *43*, 333–344.

Smith, D. M., Dunstone, N. J., Scaife, A. A., Fiedler, E. K., Copsey, D., & Hardiman, S. C. (2017). Atmospheric response to Arctic and Antarctic sea ice: The importance of ocean-atmosphere coupling and the background state. *Journal of Climate*, *30*(12), 4547–4565.

Smith, D. M., Screen, J. A., Deser, C., Cohen, J., Fyfe, J. C., García-Serrano, J., et al. (2019). The Polar Amplification Model Intercomparison Project (PAMIP) contribution to CMIP6: Investigating the causes and consequences of polar amplification. *Geoscientific Model Development*, *12*(3), 1139–1164.

Stroeve, J., & Notz, D. (2018). Changing state of Arctic sea ice across all seasons. *Environmental Research Letters*, *13*(10). https://doi.org/10.1088/1748-9326/aade56

Sun, L., Alexander, M., & Deser, C. (2018). Evolution of the global coupled climate response to Arctic sea ice loss during 1990–2090 and its contribution to climate change. *Journal of Climate*, *31*(19), 7823–7843.

Sun, L., Deser, C., & Tomas, R. A. (2015). Mechanisms of stratospheric and tropospheric circulation response to projected Arctic sea ice loss. *Journal of Climate*, *28*(19), 7824–7845.

Sun, L., Perlwitz, J., & Hoerling, M. (2016). What caused the recent "warm Arctic, cold continents" trend pattern in winter temperatures? *Geophysical Research Letters*, *43*, 5345–5352. https://doi.org/10.1002/2016GL069024

Taylor, K. E., Stouffer, R. J., & Meehl, G. A. (2012). An overview of CMIP5 and the experiment design. *Bulletin of the American Meteorological Society*, *93*, 485–498.

Tomas, R. A., Deser, C., & Sun, L. (2016). The role of ocean heat transport in the global climate response to projected Arctic sea ice loss. *Journal of Climate*, *29*(19), 6841–6859.

Vavrus, S. J. (2018). The influence of Arctic amplification on mid-latitude weather and climate. *Current Climate Change Reports*, *4*(3), 238–249.

Wang, K., Deser, C., Sun, L., & Tomas, R. A. (2018). Fast response of the tropics to an abrupt loss of Arctic sea ice via ocean dynamics. *Geophysical Research Letters*, *45*, 4264–4272. https://doi.org/10.1029/2018GL077325

Webb, M. J., Andrews, T., Bodas-Salcedo, A., Bony, S., Bretherton, C. S., Chadwick, R., et al. (2017). The Cloud Feedback Model Intercomparison Project (CFMIP) contribution to CMIP6. *Geoscientific Model Development*, *10*(1), 359–384. https://doi.org/10.5194/gmd-10-359-2017

Zappa, G., Pithan, F., & Shepherd, T. G. (2018). Multimodel evidence for an atmospheric circulation response to Arctic sea ice loss in the CMIP5 future projections. *Geophysical Research Letters*, *45*, 1011–1019. https://doi.org/10.1002/2017GL076096